



Full Length Article

Transcriptome Analysis of *Aconitum carmichaelii* Identifies Genes Involved in Terpenoid, Alkaloid and Phenylpropanoid Biosynthesis

Jihai Gao^{1†}, Dayan Zhang^{2†}, Feixia Hou¹, Huan Wen¹, Qihao Wang¹, Mingwang Song³ and Cheng Peng^{1*}

¹State Key Laboratory Breeding Base of Systematic Research, Development and Utilization of Chinese Medicine Resources, Chengdu University of Traditional Chinese Medicine, Chengdu 611137, Sichuan, PR China

²Ya'an Xun Kang medicine co., LTD., Ya'an 625600, Sichuan, PR China

³Xiajin NO. 1 Senior High School, Dezhou City 253213, Shandong, PR China

*For correspondence: peng_cutcm@126.com

†Co-first authors

Abstract

In this study, RNA sequencing of six *Aconitum carmichaelii* organs was performed using the Illumina HiSeq 2500 high-throughput platform. The *de novo* assembly yielded 103,338 unigenes, a total of 19,807 unigenes were annotated and 12,061 were assigned to 129 specific metabolic pathways by KEGG. Importantly, 382 unigenes were identified as being involved in the biosynthesis of phenylpropanoids (183 unigenes), alkaloids (42 unigenes) and terpenoids (158 unigenes). Then a comprehensive skeleton of the terpenoid-alkaloids secondary metabolism of *A. carmichaelii* was generated. Subsequently, the expression of many secondary metabolism genes was verified via the QRT-PCR method, which further demonstrated that these important genes participating in the three main secondary metabolites of *A. carmichaelii*. This study produced the first transcriptomic dataset and provided a comprehensive pathway network for the terpenoid-alkaloids secondary metabolites of *A. carmichaelii* plants, allowing us to efficiently identify candidate genes involved in the biosynthetic pathways of phenylpropanoids, alkaloids and especially AC, HA and MA. The results also provided a better understanding of the molecular mechanisms responsible for the quality of this medicinal material. © 2019 Friends Science Publishers

Keywords: *Aconitum carmichaelii*; Transcriptome; Terpenoid; Alkaloid; Phenylpropanoid; Expression patterns

Introduction

Aconitum carmichaelii Debx. is one of the most widely used Chinese traditional medicinal herbs and has been clinically used for almost two thousand years (Singhuber *et al.*, 2009; Tai *et al.*, 2015). Fuzi, the lateral root (LR) of *A. carmichaelii* Debx., has been extensively used as a cardiotoxic, analgesic, anti-inflammatory, and diuretic agent to treat colds, polyarthralgia, diarrhoea, heart failure, beriberi, and edema, while the tap roots (TR) (also referred to as mother roots, or main roots) are referred to as “Chuanwu” and are used for the clinical treatment of pains and rheumatics (Zhou *et al.*, 2015; Gao *et al.*, 2018).

During the past decades, various bioactive ingredients in *A. carmichaelii*, such as flavonoids, saponines, glucides, fatty acids, ceramides and glycosides, have been thoroughly investigated (Liu *et al.*, 2012; Ding *et al.*, 2014; Zhou *et al.*, 2015). Multiple aconitine alkaloids, such as norditerpenoid alkaloids and diterpenoid-alkaloids (C₁₉-diterpenoid and C₂₀-diterpenoid alkaloids), were identified individually and demonstrated to be the main pharmaceutical ingredients (Shim *et al.*, 2005). The diterpenoid-alkaloids originating from *A. carmichaelii* include aconitine (AC), mesaconitine

(MA) and hypaconitine (HA) as well as their demethyl derivatives (Ding *et al.*, 1993; Facchini, 2006; Zhang *et al.*, 2012; Zhang *et al.*, 2015a). Although these compounds can be synthesized using chemical methods *in vitro*, their biosynthesis pathway *in vivo* remains poorly understood. The biosynthetic pathways of terpenoid skeletons are also not well understood in the medicinal plants *Catharanthus roseus* and *Andrographis paniculata* (Zhu *et al.*, 2014; Garg *et al.*, 2015) and this is also true in *A. carmichaelii*. In addition, with standardized and concentrated agricultural bases of *A. carmichaelii* emerging sequentially, the quality standardization process of Chinese medicine was advanced. Research on the secondary metabolic pathway of *A. carmichaelii* is important for promoting its development. It not only provides a theoretical basis for maintaining the bioactive products of raw medicinal materials from different bases at content uniform levels represents in this industry, but also guides the scientific management of *A. carmichaelii* cultivation according to the secondary metabolic pathway.

Thus, it remained largely non-existent until now in *A. carmichaelii* for its biosynthetic pathways and gene regulation patterns of these bioactive molecules. In our research, we established multiple transcriptomic databases

from the flowers, fruits, leaves, stems and lateral and main roots of *A. carmichaelii* using next-generation sequencing technology. On this basis, functional annotation and enrichment analysis of transcripts was carried out to explore the key regulation genes and metabolite pathways, which involved in the biosynthesis of phenylpropanoids, alkaloids and terpenoids. This study produced the first transcriptomic dataset and provided a comprehensive pathway network for the terpenoid-alkaloids secondary metabolites of *A. carmichaelii* plants.

Materials and Methods

Plant Materials

The whole healthy *A. carmichaelii* plants, which had been grown for 10 months, were harvested (with root surface soil) from the Jiangyou GAP (Good Agricultural Practices for Medicinal Plants and Animals) plantation bases in Sichuan province, China. The Jiangyou GAP bases is a core and Daodi (genuineness) area for cultivating *A. carmichaelii* crops in accordance with the GAP manuals (<http://www.scst.gov.cn/zhuzhan/kjbfq/20041011/19254.htm>). After washing by distilled water and 70% ethyl alcohol successively, the flowers (FL), fruits (FR), leaves (L), stems (S) and lateral and main roots (LR and TR) of five whole plants were mixed (Fig. 1). The roots were all used for total RNA extraction. For the stem and leaf samples, the tip, middle and bottom portions from five plants were mixed in equal parts. The flower and fruit samples contained equal amounts of materials from different developmental stages. All organ samples were washed with water and 75% ethyl alcohol, followed by freezing in liquid nitrogen before RNA extraction and high-performance liquid chromatography (HPLC) detection.

RNA Isolation, Transcriptome Sequencing and De Novo Assembly

Total RNA was extracted from each organ using the TRIzol reagent (Invitrogen, Burlington, ON, Canada). The cDNA libraries were generated according to the Illumina protocol (Zhang *et al.*, 2018) and then paired-end sequenced with an Illumina HiSeq™ 2500 system. The raw read datasets in FASTQ format were first processed using in-house Perl scripts. In this step, clean data (clean reads) were obtained by removing reads containing adapter or poly-N sequences and low-quality reads from the raw data. The Q20, Q30, GC content and sequence duplication levels of the clean data were calculated simultaneously. All of the downstream analyses were based on clean data with high quality. Transcriptome assembly was carried out based on the complete paired end sequences (FASTQ files) using Trinity software by default, and all other parameters were set to the defaults.

Functional Annotation and Differential Expression Analysis

All assembled unigenes were annotated by matching against the NCBI non-redundant protein sequence (NR), Clusters of Orthologous Groups (COG), euKaryotic Orthologous Groups (KOG), Gene Ontology (GO), Protein family (Pfam), Swiss-Prot protein (Swiss-prot), and Kyoto Encyclopaedia of Genes and Genomes (KEGG) databases, using BLASTx with an E-value threshold of $1E-5$. The NR annotations were then used to calculate similarity, E-value, and species distributions from the BLAST results.

Prior to differential gene expression analysis, for each sequenced library, the read counts were adjusted using the edgeR programme package (Robinson *et al.*, 2010) through one scaling-normalized factor. Gene expression levels were estimated for each sample with RSEM (Li and Dewey, 2011). Differential expression analysis of two samples was performed using the DEGseq R package (Wang *et al.*, 2010). Fragments per kilobase of transcript per million fragments mapped (FPKM) values were calculated to estimate the expression level of each unigene (Mortazavi *et al.*, 2008). A false discovery rate (FDR) ≤ 0.05 and an estimated absolute \log_2 fold-change (\log_2FC) $\geq C$ -change (logiminated absolute logpression indicated a significant difference in gene expression between two samples.

GOseq R packages and KOBAS were employed to conduct GO and KEGG enrichment analysis of the differentially expressed genes (DEGs) (Young *et al.*, 2010). Significantly enriched functional categories and pathways were identified among the DEGs based on comparison with the whole transcriptome background.

High-Performance Liquid Chromatography (HPLC) Detection

To evaluate the content of aconitine-type alkaloids in different organs of *A. carmichaelii* plants, HPLC detection was performed on the Shimadzu LC-20AT system, using an Agilent 5 Tc-C₁₈ (2) (250 × 4.6 mm) chromatographic column. For sample preparation, approximately 1 g of dry organ powder and 3 mL of ammonia water were mixed and an isopropanol-ethyl acetate (1:1) solution was then added to obtain a total volume of 20 mL. After the sample was weighed out, ultrasonic processing was performed for 30 min, followed by replenishing with isopropanol-ethyl acetate (1:1). Then, 10 mL of the filtrate was isolated and dried under conditions of low temperature and hypopiesia. The remaining material was re-dissolved with 3 mL of an isopropanol-dichloromethane (1:1) solution. After filtration with a 0.45 μm microporous membrane, the test solution was obtained, and 10 μL of the extract solution was employed for HPLC.

The mobile phase (A phase) consisted of acetonitrile-tetrahydrofuran (25:15) and (B phase) 0.1 mol/L ammonium

acetate. The programme settings were as follows: 15%-26% over 0-48 min, 26%-35% over 48-53 min, 35% over 53-63 min and 35%-15% over 63-70 min for mobile phase A, with a detection wavelength of 235 nm. For the detection of references and standard curves, mesaconitine (MA), hyaconitine (HA), aconitine (AC), benzoylmesaconine, benzoylaconine and benzoylhyaconitine were prepared with a dichloromethane-isopropanol (1:1) solution.

Validation of Gene Expression via QRT-PCR

Quantitative real-time PCR (QRT-PCR) was performed to quantify some of the DEGs based on transcriptome data and their expression patterns in response to environmental stresses. Total RNA was extracted, and reverse transcribed into cDNA using the methods mentioned above. The genes were distributed among the three backbone pathways of secondary metabolites in plants, particularly the diterpenoid-alkaloid biosynthesis pathway. Their sequences and information were exported from the *A. carmichaelii* transcriptome with the QRT-PCR primers designed for these analyses.

These assays were conducted on a Bio-Rad CFX 1000 Real-Time PCR System in a 20 μ L volume containing the cDNA from each sample, 10 μ L of SsoFast™ EvaGreen Supermix (Bio-Rad, USA), 1.0 μ L of each primer and 7 μ L of double-distilled H₂O. The PCR profile included one cycle of 95°C for 20 s, 45 cycles 95°C for 5 s and T_m°C for 20 s and a final melting curve profile (65–95°C, 0.5°C/S). Quantification was performed *via* the $2^{-\Delta\Delta C_t}$ method. The data are reported as the average of three repeats, and the QRT-PCR assays were performed in triplicate.

Results

Diester Diterpenoid-Alkaloids in *A. carmichaelii* Organs

As the main active substances in *A. carmichaelii* plants, diester diterpenoid-alkaloids (DDAs, such as AC, MA and HA) and monoester alkaloids, which are hydrolysed from diester alkaloids (MDAs, such as benzoyl-AC, benzoyl-MA and benzoyl-HA), were detected via the HPLC method (Fig. 1 and 2). The results showed that the plants contained DDAs (0.01%-0.27%) and trace amounts of MDAs (less than 0.002%). In the main roots and leaves, no MDAs were detected. Regarding the total content of DDAs, the lateral roots exhibited the highest percentage composition, with the leaves exhibiting the lowest. The content distribution of terpenoids in *A. carmichaelii* plants was consistent with previous reports (Jaiswal *et al.*, 2014). Performed ANOVA and significance test showed that comparison of main roots (TR) the lateral roots (LR), stems (S) and flowers (FL) showed a significant difference ($P < 0.01$) in the content of MDAs, and compared with lateral roots (LR), the main roots (TR), stems (S), FL (flowers) and fruits (FR) showed

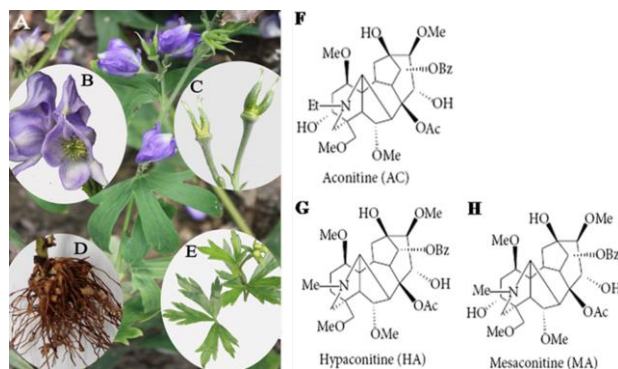


Fig. 1: *A. carmichaelii* organs for transcriptome sequencing and the chemical structures of three diterpenoid alkaloids. (A) Aconitum plant; (B) flowers (FL); (C) fruits (FR); (D) lateral and main roots (LR and TR); (E) leaves (L); (F) chemical structure of aconitine (AC); (G) chemical structure of hyaconitine (HA); (H) chemical structure of mesaconitine (MA)

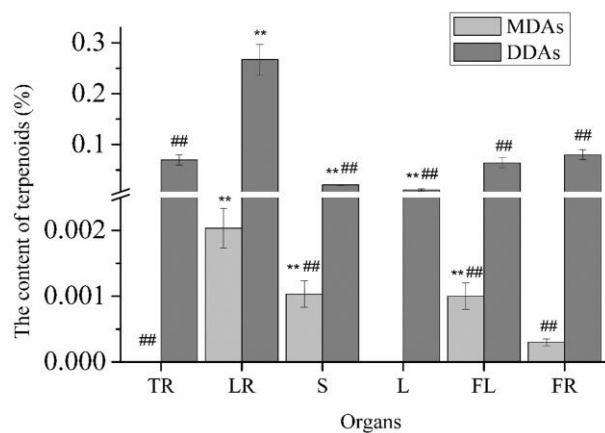


Fig. 2: Terpenoid-alkaloid content in *A. carmichaelii* organs by HPLC detection. DDAs: diterpenoid-alkaloids, including chemical structure of aconitine (AC), chemical structure of mesaconitine (MA) and chemical structure of hyaconitine (HA) added sums; MDAs: monoterpene derivatives, added up benzoyl-AC, benzoyl-MA and benzoyl-HA. TR: main roots, LR: lateral roots, S: stem, L: leaves, FR: fruits, FL: flowers, vs TR, ** $P < 0.01$, * $P < 0.05$, vs LR, ## $P < 0.01$, # $P < 0.05$

significant difference ($P < 0.01$).

Sequencing and De Novo Assembly

After removing adaptors and reads with unknown or low-quality nucleotides, 156,967,635 clean reads (28,254,174,300 bp) were obtained from the six organs (Table 1). The high-quality reads from the six libraries were subsequently *de novo* assembled into 9,836,247 contigs, 262,318 transcripts and 103,338 unigenes using the Trinity programme (Haas *et al.*, 2013). The mean length of the assembled unigenes was 653.8 bp, with an N50

Table 1: Summary of the transcriptome assembly of *Aconitum carmichaelii*

Organ	Number of reads	Number of bases	Mapped Reads	Mapped Ratio	GC Content	%≥Q30
Flower	26,187,606	4,713,769,080	21,823,905	83.34%	45.03%	93.82%
Fruit	26,007,277	4,681,309,860	21,530,964	82.79%	44.81%	93.78%
Leaf	26,008,133	4,681,463,940	22,110,562	85.01%	44.68%	93.83%
Stem	26,591,636	4,786,494,480	22,309,285	83.90%	44.33%	94.08%
Lateral root	25,727,611	4,630,969,980	21,783,541	84.67%	44.66%	93.77%
Main root	26,445,372	4,760,166,960	22,615,266	85.52%	44.95%	93.15%

value of 1,073 bp and a total size of 67,567,698 bp. In total, 76,793, 77,790, 69,274, 73,045, 71,625 and 67,087 unigenes were predicted in the transcriptomes of the flowers, fruits, leaves, stems and lateral and main roots. We have submitted the raw data to the GEO database, generating the GEO numbers SRP102756.

Functional Annotation, Classification and KEGG Pathway Analysis

A total of 38,554 unigenes (37.31%) could be matched to known genes in the public databases (Table 2), among which 52.82% showed strong homology with the matched sequences in the NR database ($<1E-45$), while 47.18% showed moderate homology (between $1E-5$ and $1E-45$). Regarding the similarity distribution, 61.74% of the matched sequences displayed a similarity higher than 60%, whereas 38.26% showed similarities between 20% and 60%. Then *A. carmichaelii* unigenes exhibited the greatest number of matches with genes of *Nelumbo nucifera* (29.93%), followed by species including *Vitis vinifera* (13.14%), *Theobroma cacao* (2.50%), *Malus domestica* (2.20%), *Setosphaeria turcica* (1.96%) and so on.

Among the 103,338 unigenes identified in the six organs, 9,954 (9.63%) were assigned to 25 COG categories. 20.46% (21,148) of the unigenes were classified to 51 GO functional terms, including 20 terms in the biological process category, 14 in the cellular component category and 17 in the molecular function category. In total, 12,061 unigenes (11.67%) were assigned to 129 KEGG pathways (Table 2). The results revealed that “ribosome” (ko03010) was the most abundant assigned pathway (512 unigenes), followed by “carbon metabolism” (ko01200, 461 unigenes), and “biosynthesis of amino acids” (ko01230, 382 unigenes).

Identification and Annotation of DEGs in Six Organs

A total of 19,807 unigenes were revealed to be differentially expressed among the six examined organs (Fig. 3). The greatest number of DEGs (8,691 unigenes) was identified in the leaves compared with the flowers, followed by the lateral roots compared with the flowers (8,173 unigenes). The greatest number of up-regulated unigenes flowers (4,544 unigenes) compared with stems.

Compared with the aboveground organs (flowers/fruits/leaves/stems), the belowground parts (lateral/main roots) exhibited 15 down-regulated

Table 2: Summary of unigene annotations for the *A. carmichaelii* transcriptomes

Database	Number of annotated unigenes	Percent of annotated unigenes
COG	9,954	9.63%
KOG	21,444	20.75%
GO	21,148	20.46%
Pfam	24,364	23.58%
Swiss-prot	22,409	21.69%
KEGG	12,061	11.67%
Nr	37,609	36.39%
All	38,554	37.31%

COG, KOG, GO, Pfam, Swiss-prot, KEGG and Nr denote the Clusters of Orthologous Groups (COG), euKaryotic Orthologous Groups (KOG), Gene Ontology (GO), Protein family (Pfam), Swiss-Prot protein (Swiss-prot), Kyoto Encyclopaedia of Genes and Genomes (KEGG), and NCBI non-redundant protein (Nr) databases

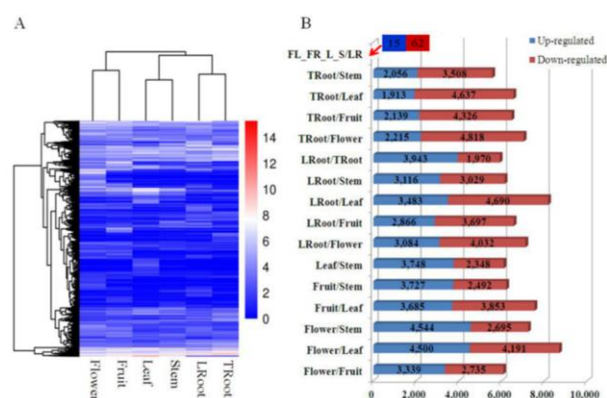


Fig. 3: Expression of all DEGs among six organs in *A. carmichaelii*. (A) Heat-map of the total 19,807 DEGs among the six organs. Samples are displayed below the heat maps. The colour scale indicates expression levels (\log_2 ratio of FPKM) ranging from low (blue) to high (red). (B) The numbers of up- and down-regulated genes in all 16 comparisons among the six organs. FL_FR_L_S/LR_TR denotes the comparison between aboveground parts (flowers, fruits, leaves and stems) and belowground parts (lateral and main roots)

unigenes, such as the abscisic stress ripening protein ($\log_2FC = -6.8$), chlorophyll a-b binding protein ($\log_2FC = -6.1$) and serine/threonine protein phosphatase 2A regulatory subunit B (specifically expressed in aboveground organs) (Fig. 3B). These unigenes were enriched in several functional categories related to photosynthesis, photosystem, chlorophyll binding and electron carrier activity (GO:0009055).

Table 3: Number of unigenes related to secondary metabolites in *A. carnichaelii*

Secondary metabolites biosynthesis pathways	Pathway ID	All	Flower	Fruit	Leaf	Stem	LRoot	TRoot
Phenylpropanoid biosynthesis	ko00940	183	146	150	145	137	139	127
Terpenoid backbone biosynthesis	ko00900	62	57	59	59	58	55	58
Cutin, suberin and wax biosynthesis	ko00073	43	32	38	26	25	31	19
Diterpenoid biosynthesis	ko00904	42	34	33	35	36	34	31
Steroid biosynthesis	ko00100	41	36	36	35	34	34	34
Ubiquinone and other terpenoid-quinone biosynthesis	ko00130	40	37	35	34	31	33	29
Carotenoid biosynthesis	ko00906	37	35	32	37	33	32	33
Tropane, piperidine and pyridine alkaloid biosynthesis	ko00960	35	25	25	32	24	22	25
Isoquinoline alkaloid biosynthesis	ko00950	31	24	24	25	20	19	20
Zeatin biosynthesis	ko00908	27	25	25	22	21	22	16
Brassinosteroid biosynthesis	ko00905	26	24	23	20	18	21	17
Flavonoid biosynthesis	ko00941	26	24	22	18	21	18	14
Nicotinate and nicotinamide metabolism	ko00760	22	18	17	21	17	17	17
Sesquiterpenoid and triterpenoid biosynthesis	ko00909	8	6	6	5	6	7	6
Monoterpenoid biosynthesis	ko00902	6	6	6	6	6	5	6
Anthocyanin biosynthesis	ko00942	6	5	5	6	6	6	6
Caffeine metabolism	ko00232	5	3	3	5	3	3	3
Flavone and flavonol biosynthesis	ko00944	5	4	3	2	3	3	3

LRoot and TRoot denote lateral and main roots, respectively

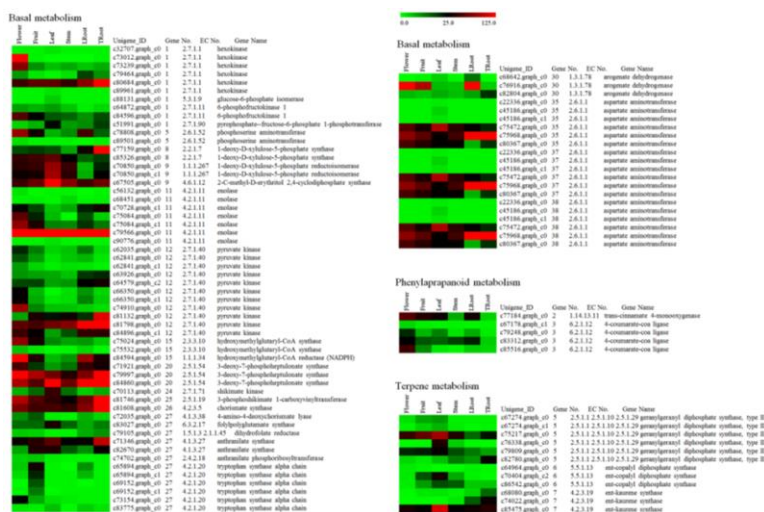


Fig. 4: The expression heatmaps of some key DEGs. The genes were mapped using FPKM values and are colour coded according to increasing relative expression

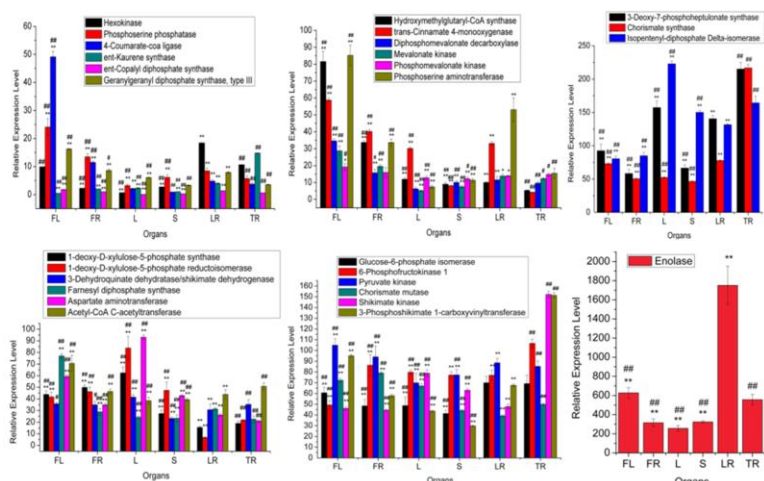


Fig. 5: QRT-PCR confirmation of selected genes involved in terpenoid, alkaloid and phenylpropanoid biosynthesis. TR: main roots, LR: lateral roots, S: stems, L: leaves, FR: fruits, FL: flowers, vs TR, * $P < 0.01$, * $P < 0.05$, vs LR, ## $P < 0.01$, #

In the roots compared with aboveground organs, a total of 62 unigenes were found to be up-regulated, including 9 tissue-specific sequences, *ent*-kaurene synthase ($\log_2FC = 5.0$), and a pathogen-related protein-like sequence ($\log_2FC = 5.9$). The greatest number of unigenes were involved in the photosynthesis antenna protein (ko00196) and plant hormone signal transduction (ko04075) pathways. *ent*-Kaurene synthase is a key enzyme to catalyze diterpene synthesis and was found to show the highest expression in the roots of *A. carmichaelii*, especially in the lateral roots. The observation that the pathogen-related protein-like gene was detected at the highest level in the roots, followed by the stems, leaves, flowers (undetectable) and fruits (undetectable) is worthy of further study. The transcription level of this gene seemed to be affected by soil microbes.

In comparison with the main roots, the lateral roots exhibited 3943 up-regulated unigenes (Fig. 3B), including 9 that were relevant to phenylpropanoid biosynthesis (GO:0009698), such as AMP-dependent CoA ligase ($\log_2FC = 2.5$) and caffeic acid 3-O-methyltransferase ($\log_2FC = 2.6$); and 3 that were relevant to terpenoid metabolic pathways (GO:0043693, 2 limonene synthases and 1 monoterpene synthase-like gene). Additionally, 1970 sequences were down-regulated in the lateral roots compared with the main roots, such as caffeic acid 3-O-methyltransferase ($\log_2FC = -3.2$) and ferrihemoprotein oxidoreductase ($\log_2FC = -1.7$). The 5913 total DEGs were distributed among secondary pathways such as linoleic acid metabolism (ko00591), phenylalanine metabolism (ko00360) and phenylpropanoid biosynthesis (ko00940). Thus, the DEGs were assumed to be associated with the differential contents of aconite-alkaloids between the lateral roots and main roots (Fig. 2).

In the *A. carmichaelii* transcriptomes, a total of 645 unigenes, including 337 DEGs, were involved in 18 secondary metabolic pathways, among which 8 participated in the biosynthesis of phenylpropanoids, alkaloids and terpenoids (Table 3). Notably, “phenylpropanoid biosynthesis” (ko00940) was the most abundant, which contained 183 unigenes and 107 DEGs. This pathway is responsible for the biosynthesis of compounds such as lignans, lignins, isoflavonoids, stilbenoids, flavones and flavonols and styrylpyrones. The heatmaps of some key and typical DEGs are indicated in the secondary metabolism (Fig. 4). Among all of the unigenes participating in the three main secondary metabolites, 28 were selected for verification of their transcriptional abundance via the QRT-PCR method (Fig. 5). The results were mostly consistent with the transcriptome data.

Genes Related to Phenylpropanoid Biosynthesis

A total of 183 predicted unigenes were involved in the *A. carmichaelii* phenylpropanoid biosynthesis pathway (ko00940), among which 107 were differentially expressed between the lateral/main roots and

flowers/fruits/leaves/stems in *A. carmichaelii* (Table 3). The three most abundant genes were peroxidase (66 unigenes), beta-glucosidase (40 unigenes) and caffeic acid 3-O-methyltransferase (21 unigenes) (Table 4).

Among these 107 DEGs, 42 (39.25%) were down-regulated in both the lateral and main roots compared with the flowers, fruits, leaves and stems, while 77 DEGs (71.97%) were down-regulated in either the lateral or main roots. Additionally, 25 DEGs were up-regulated in either the lateral or main roots, and the up-regulated DEGs encoded nine proteins: beta-glucosidase, cinnamyl-alcohol dehydrogenase (CAD), cinnamoyl-CoA reductase (CCR), caffeic acid 3-O-methyltransferase (COMT), CYP98A, shikimate O-hydroxycinnamoyl transferase (HCT), phenylalanine ammonia-lyase (PAL), peroxidase and coniferyl-aldehyde dehydrogenase (REF1). These data suggested that the majority of the DEGs participating phenylpropanoid pathways accumulated in aboveground organs and were down-regulated in the roots, as can be observed for 4-coumarate-CoA ligase and trans-cinnamate 4-monooxygenase in Table 4 and Fig. 4. This pattern may have been due to the greater biomass of secondary metabolites in the aboveground parts than in the roots, as observed for compounds such as lignin, flavonoids, coumarins, and lignans.

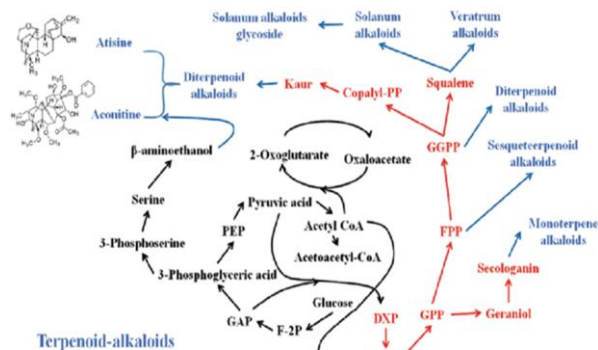
Candidate Genes Involved in Alkaloid Biosynthesis

In the present study, two pathways involved in alkaloid biosynthesis were identified in the obtained transcriptomes (Table 3). Interestingly, all of the DEGs in alkaloid biosynthetic pathways were down-regulated in the lateral or main roots compared with the four aboveground organs. Among these DEGs, 11 were down-regulated in the roots. In contrast, only seven unigenes were up-regulated in the lateral roots compared with the fruits, leaves and stems. These unigenes encoded tyrosine aminotransferase (c75243.graph_c0, c75243.graph_c1, and c75243.graph_c1), tyrosine decarboxylase (c83329.graph_c1), primary-amine oxidase (c64923.graph_c0 and c84424.graph_c0) and aspartate aminotransferase (c75968.graph_c0).

22 alkaloid biosynthesis unigenes were expressed in all six organs, suggesting that these genes might be expressed in the whole *A. carmichaelii* plant to generate alkaloids. This finding provides clues regarding the biosynthetic mechanisms of AC, HA and MA. We found that the expression levels of seven unigenes (c74325.graph_c0, c75968.graph_c0, c79358.graph_c0, c84448.graph_c0, c84800.graph_c0, c100659.graph_c0 and c108873.graph_c0) were higher in belowground parts than in aboveground parts. These unigenes encoded aminotransferase, amine oxidase, and tropinone reductase. Further investigation is necessary to determine whether the expression of these unigenes could result in the alkaloid content difference observed between aboveground and belowground parts.

Table 4: Predominant gene families encoded by unigenes involved in terpenoid, alkaloid, and phenylpropanoid biosynthesis in *A. carmichaelii*

Secondary metabolites biosynthesis pathways	Pathway ID	Enzyme ID	Function	Number of Genes		
Terpenoid backbone biosynthesis	ko00900	EC:2.2.1.7	1-deoxy-D-xylulose-5-phosphate synthase	9		
		EC:2.5.1.1	geranylgeranyl diphosphate synthase, type II	8		
		EC:2.5.1.10				
		EC:2.5.1.29				
Diterpenoid biosynthesis	ko00904	EC:3.1.1.-	prenylcysteine alpha-carboxyl methylesterase	6		
		EC:5.5.1.13	ent-copalyl diphosphate synthase	8		
		EC:4.2.3.19	ent-kaurene synthase	7		
		EC:1.14.13.79	ent-kaurenoic acid hydroxylase	8		
		EC:6.2.1.12	4-coumarate-CoA ligase	9		
Ubiquinone and other terpenoid-quinone biosynthesis	ko00130	EC:6.2.1.12	4-coumarate-CoA ligase	9		
Isoquinoline alkaloid biosynthesis	ko00950	EC:2.6.1.1	aspartate aminotransferase, chloroplasmic	2		
			aspartate aminotransferase, cytoplasmic	4		
			aspartate aminotransferase, mitochondrial	2		
		EC:2.6.1.1	bifunctional aspartate aminotransferase and glutamate/aspartate-prephenate aminotransferase	3		
		EC:2.6.1.78				
		EC:2.6.1.79				
		EC:1.4.3.21	primary-amine oxidase	9		
		EC:1.14.18.1	Tyrosinase	1		
		EC:2.6.1.5	tyrosine aminotransferase	4		
		EC:4.1.1.25	tyrosine decarboxylase	6		
		Tropane, piperidine and pyridine alkaloid biosynthesis	ko00960	EC:2.6.1.1	aspartate aminotransferase, chloroplasmic	2
					aspartate aminotransferase, cytoplasmic	4
					aspartate aminotransferase, mitochondrial	2
				EC:2.6.1.1	bifunctional aspartate aminotransferase and glutamate/aspartate-prephenate aminotransferase	3
EC:2.6.1.78						
EC:2.6.1.79						
EC:2.6.1.9	histidinol-phosphate aminotransferase			1		
EC:1.4.3.21	primary-amine oxidase			9		
EC:1.1.1.206	tropinone reductase 1			9		
EC:2.6.1.5	tyrosine aminotransferase			4		
Phenylpropanoid biosynthesis	ko00940	EC:3.2.1.21	beta-glucosidase	40		
		EC:2.1.1.68	caffeic acid 3-O-methyltransferase	21		
		EC:1.11.1.7	peroxidase	66		

**Fig. 6:** Biosynthetic pathway of terpenoid-alkaloids. IPP: isopentenyl-diphosphate, GPP: geranyl diphosphate, FPP: farnesyl pyrophosphate, GGPP: geranylgeranyl diphosphate, HMG-CoA: hydroxymethylglutaryl-CoA synthase, DXP: 1-deoxy-D-xylulose-5-phosphate synthase

Identification of Genes Related to Terpenoid Biosynthesis

Terpenes and terpene-alkaloids, particularly the DDAs and their derivatives, are important pharmacological metabolites. According to the comprehensive, simplified illustration of the network skeleton regarding terpenoid-alkaloids

secondary metabolites (Fig. 6), the relative gene expression, transcriptional regulation and metabolite biosynthesis were studied and further discussed in *A. carmichaelii*.

In this study, five pathways were found to take part in the biosynthesis of these compounds (Table 3 and 5). In total, 158 unigenes were functionally annotated in these five pathways, including terpenoid backbone biosynthesis (ko00900), diterpenoid biosynthesis (ko00904), monoterpene biosynthesis (ko00902), sesquiterpenoid and triterpenoid biosynthesis (ko00909) and ubiquinone and other terpenoid-quinone biosynthesis (ko00130). Among which 70 were differentially expressed between the lateral/main roots and flowers/fruits/leaves/stems in *A. carmichaelii*. In terpenoid backbone biosynthesis (ko00900) pathways, 14 DEGs were up-regulated in the lateral root compared with the leaves, and 12 DEGs were up-regulated in the main roots compared with the leaves. Additionally, in ubiquinone and other terpenoid-quinone biosynthesis (ko00130) pathways, compared with the leaves, 12 DEGs were up-regulated in the main roots, and the up-regulated DEGs mainly encoded trans-cinnamate-4-monooxygenase (c77184.graph_c0), tyrosineaminotransferase (c75885.graph_c0, c75243.graph_c0, c75243.graph_c1, c77943.graph_c0), 4-coumarate-CoA ligase (c79248.graph_c0, c83312.graph_c0).

Table 5: Expression of unigenes related to diterpenoid biosynthesis in *A. carmichaelii*

Unigene ID	Gene Name	FPKM						
		Flower	Fruit	Leaf	Stem	LRoot	TRoot	
MEV pathway								
c107977.graph_c0	AACT	0	0	1.139343	0	0	0	
c75090.graph_c0	AACT	70.53833	46.37347	38.4303	39.31368	43.85119	50.7620871	
c1140.graph_c0	HMGs	1.767217	0.895253	0	0	0.14761	0	
c75024.graph_c0*	HMGs	81.5582	33.71047	11.94566	9.012139	10.02447	5.3246905	
c75532.graph_c0*	HMGs	5.525981	2.190836	0.473821	0.822405	3.732672	0.58104203	
c84594.graph_c0*	HMGR	238.4287	38.80798	6.875636	10.22911	84.51017	36.0662808	
c77006.graph_c0	MK	28.69949	19.5494	5.148248	7.516496	13.78171	12.265735	
c81407.graph_c0	PMK	19.21414	15.92159	12.75701	12.23313	13.87262	14.6991599	
c81256.graph_c0	MVD	34.67154	15.70032	6.302699	10.05963	11.57502	9.63844048	
MEP pathway								
c103180.graph_c0	DXS	0	0.655024	0.212497	0	0	0	
c114230.graph_c0	DXS	0	0.287896	0	0.277899	0	0.27487554	
c60429.graph_c0	DXS	0.877533	0.790308	0.67301	0.667506	0.488649	0.56592393	
c64071.graph_c0	DXS	26.22159	13.04205	8.344443	7.809933	7.2874	10.6074276	
c64071.graph_c1	DXS	23.42378	13.05285	8.950172	6.777044	7.434741	11.5183832	
c77159.graph_c0*	DXS	17.6329	19.15451	17.46673	8.612557	32.99921	161.467704	
c80667.graph_c0	DXS	13.20383	9.604593	5.656728	4.856271	12.3861	11.7902693	
c85326.graph_c0*	DXS	43.89411	49.92063	62.35066	27.38522	15.49041	18.9380006	
c94609.graph_c0	DXS	0	0	0	0.518541	0	0.25644996	
c70850.graph_c0*	DXR	41.74773	46.22143	83.72843	47.38754	6.721642	21.7457034	
c70850.graph_c1*	DXR	30.47778	32.94517	88.73745	41.80556	7.786872	27.7485558	
c79785.graph_c0	CMK	10.02974	14.25795	11.68531	9.446849	4.887311	4.68696828	
c67505.graph_c0*	MDS	47.62622	65.82905	157.1818	78.70104	51.28612	68.064644	
c80598.graph_c0*	HDR	72.30685	66.66632	353.642	114.3962	50.31411	98.3823063	
c83362.graph_c0	HDS	72.34678	69.36133	209.9289	71.22164	70.94232	135.30219	
MEV/MEP pathway								
c72994.graph_c0	IDI	80.53874	84.97534	222.9782	150.1932	131.6561	164.31836	
Diterpenoid biosynthesis (ko00904)								
c110247.graph_c0	CPS	0	0	0	0	0.871959	0	
c15201.graph_c0	CPS	0.536214	0	0	0.262207	0.268729	0.51870965	
c19203.graph_c0	CPS	0.472003	0.717334	0	0.230808	0.236549	0	
c19721.graph_c0	CPS	0	0	0	0	0.702606	0.67809577	
c35028.graph_c1	CPS	1.636352	0.276319	0	0	0	0	
c57031.graph_c0	CPS	0.486557	1.478905	0	0.237925	0.731528	0	
c59188.graph_c0	CPS	1.12248	0.812337	0.316237	0.313651	1.125084	0.46535848	
c64964.graph_c0*	CPS	1.785567	0.978389	0.071864	0.285106	1.296627	0.61688489	
c70404.graph_c2*	CPS	2.07215	17.02893	33.14624	8.331374	0.22272279	0.22272279	
c83647.graph_c0	CPS	5.899952	6.797224	3.331101	4.187989	5.007519	5.062971	
c86542.graph_c0*	CPS	1.495945	9.575392	17.52753	16.1277	5.080373	5.43091761	
c91756.graph_c0	CPS	0	0	0	0.174731	1.074466	0.17283071	
c31406.graph_c0	KS	0	0	2.005632	1.193537	1.630966	0.59027677	
c39955.graph_c0	KS	0	0.436683	0.424994	0.210759	0	0	
c68080.graph_c0*	KS	0.466959	2.010726	2.302242	1.027536	3.978357	14.7936586	
c71383.graph_c0	KS	14.99466	10.49647	10.48434	13.0649	9.290933	15.032622	
c74022.graph_c0*	KS	0.234412	0.356251	0.154096	2.025069	16.17277	28.949599	
c85202.graph_c0	KS	21.53134	17.45991	18.51999	11.93007	6.753859	14.1603503	
c85475.graph_c0*	KS	35.75794	27.73493	109.9743	26.58545	31.321	40.918928	
c86325.graph_c0	KS	4.585364	4.286796	2.425134	3.404112	6.183713	8.04470211	
c68883.graph_c0*	KO	16.67359	11.92163	32.70495	32.58822	56.93505	160.323613	
c71637.graph_c0	KO	18.23256	25.7109	26.00279	19.9881	19.20884	26.0504089	
c84702.graph_c0*	KO	16.85614	13.98048	56.65345	11.49284	8.634167	13.7596907	
c117118.graph_c0	KA0	0	0	0.519905	0	0	0	
c42691.graph_c0	KA0	0	0	0.347065	0.344227	0	0	
c55237.graph_c0	KA0	0.639601	0.810036	0.315342	0.547335	0.72122	1.77882243	
c71933.graph_c0*	KA0	11.59945	11.15297	9.332788	23.14115	67.9021	102.081815	
c75104.graph_c0	KA0	5.092906	4.317567	4.509464	4.269284	3.64623	3.31794714	
c78753.graph_c0*	KA0	1.667048	3.229001	7.203741	1.150844	14.5468	7.30425323	
c78983.graph_c0*	KA0	0.738382	19.56905	0.421525	0.114021	1.363334	0	
c85327.graph_c0	KA0	15.97921	32.37957	8.765172	14.23041	10.60681	12.130613	
c74424.graph_c0*	GA20ox	6.646058	0.342388	0.360992	0.71608	1.693596	0.05448389	
c88225.graph_c0	GA20ox	1.987706	0.359625	0.349999	0.485991	1.138467	0.27468818	
c69947.graph_c0*	GA3ox	0	0.746375	4.277671	1.040659	0.246125	2.89006505	
c81220.graph_c0*	GA3ox	6.329009	3.373694	11.55009	4.064899	3.053494	3.63231887	
c101583.graph_c0	GA2ox	0.20518	0.207884	0.202319	0.401329	0.205656	0	
c23758.graph_c0	GA2ox	0.236001	0.239111	0.930844	0.692423	0	0.22829703	
c3807.graph_c0	GA2ox	0.742918	0	0.18314	0	0	0	
c4789.graph_c0	GA2ox	0.594785	0	0.390996	0	0	0	
c60147.graph_c0*	GA2ox	2.951109	0.92	0.149229	0.296017	0.45507	0.21959775	
c65289.graph_c0*	GA2ox	3.872113	2.65077	1.754276	0.614093	3.041941	4.25188552	
c73711.graph_c0*	GA2ox	2.24448	14.44226	11.72601	6.046119	3.749479	0.34282246	

LRoot and TRoot denote lateral and main roots, respectively

The MEV and MEP pathways are the cytosolic mevalonic acid (MEV) pathway and the plastidial 2C-methyl-D-erythritol-4-phosphate (MEP) pathway, both of which are responsible for the terpenoid building blocks isopentenyl diphosphate (IPP) and dimethylallyl diphosphate (DMAPP)

* Denotes unigenes that were differentially expressed between the lateral/main roots and flowers/fruits/leaves/stems

Abbreviations: AACT, acetyl-CoA C-acetyltransferase; HMGs, hydroxymethylglutaryl-CoA synthase; HMGR, hydroxymethylglutaryl-CoA reductase; MK, mevalonate kinase; PMK, phosphomevalonate kinase; MVD, diphosphomevalonate decarboxylase; DXS, 1-deoxy-D-xylulose-5-phosphate synthase; DXR, 1-deoxy-D-xylulose-5-phosphate reductoisomerase; CMK, 4-diphosphocytidyl-2-C-methyl-D-erythritol kinase; MDS, 2-C-methyl-D-erythritol 2,4-cyclodiphosphate synthase; HDR, 4-hydroxy-3-methylbut-2-enyl diphosphate reductase; HDS, (E)-4-hydroxy-3-methylbut-2-enyl-diphosphate synthase; IDI, isopentenyl-diphosphate delta-isomerase; CPS, *ent*-copalyl diphosphate synthase; KS, *ent*-kaurene synthase; KO, *ent*-kaurene oxidase; KAO, *ent*-kaurenoic acid hydroxylase; GA20ox, gibberellin 20-oxidase; GA3ox, gibberellin 3-beta-dioxygenase; GA2ox, gibberellin 2-oxidase

Discussion

In recent years, large-scale omics analyses of many TCM plants have been performed, and the sequences have been released to the public. For the *A. carmichaelii* transcriptome in this paper, despite the large amounts of raw data, the low COG, GO and KEGG annotation ratios are similar to those of other herbal plants, such as *Codonopsis pilosula* (Gao *et al.*, 2015) and *Isatis indigotica* (Tang *et al.*, 2014). However, deep functional annotations and verification analyses of the novel hypothetical genes are less. Nevertheless, we tried to predict some key genes regulating the DDAs biosynthesis in *A. carmichaelii*. Interestingly, only 9 DEGs in ubiquinone and other terpenoid-quinone biosynthesis (ko00130) pathways were down-regulated in the main roots compared with the fruits, and only one unigene were up-regulated in the lateral and main roots compared with the four aboveground organs. These unigenes comprised almost all known terpene biosynthesis pathway genes, such as diphosphomevalonate decarboxylase, farnesyl diphosphate synthase (FPS), geranylgeranyl diphosphate synthase (GGPPS), *ent*-copalyl diphosphate synthase (CPS), *ent*-kaurene synthase (KS or KSL), *ent*-kaurene oxidase (KO), *ent*-kaurenoic acid hydroxylase (KAO).

FPSs are indispensable enzymes for terpenoid skeleton biosynthesis. Gene silencing of *A. thaliana* FPS alters chloroplast development and plastidial isoprenoid levels and results in misregulation of genes involved in the jasmonic acid (JA) pathway and the abiotic stress response (Manzano *et al.*, 2016). Their expression profiles in plants show spatial and temporal variations. In the *A. carmichaelii* transcriptomes, one FPS unigene (c80411.graph_c0) was detected. Its highest expression occurred in the flowers, where it was 3-fold higher than that in the roots. The predominant organ showing c80411.graph_c0 transcription was consistent with findings reported for *HbFPS2* in *Hevea brasiliensis*, *MeFPS2* in *Manihot esculenta* and *RcFPS2* in *Ricinus communis* (Adiwilaga and Kush, 1996).

A total of 7 GGPPS unigenes were sequenced in the *A. carmichaelii* transcriptome, among which 4 (c67274.graph_c1, c76338.graph_c0, c79809.graph_c0 and c75217.graph_c0) showed the highest expression in leaves, 2 (c2937.graph_c0 and c82780.graph_c0) in the main roots, and 1 (c83598.graph_c0) in the flowers. The expression level of c76338.graph_c0 showed the largest difference between tissues, with a difference of 8-180-fold being observed in the leaves compared with other plant parts. Therefore, the *A. carmichaelii* GGPPS genes displayed similar locations of accumulation to IbGGPS proteins from *Ipomoea batatas* (Chen *et al.*, 2015), which were found to reside to specific areas of the plasma membrane and chloroplasts in leaves. Thus, these genes are commonly used as a source for carotenoid genetic engineering. As a homology family, GGPPSs might play multiple roles in plants. For instance, TwGGPPS4 and TwGGPPS5 of *Tripterygium wilfordii* can participate in miltiradiene

biosynthesis, while TwGGPPS1 and TwGGPPS4 are likely involved in triptolide biosynthesis (Zhang *et al.*, 2015). In *A. thaliana*, the GGPPSs were revealed to enhance osmotic stress tolerance and increase carotenoid contents (Beck *et al.*, 2013; Ruiz-Sola *et al.*, 2016) and it may be possible to exploit the various functions of GGPPs in *A. carmichaelii* through correlation analysis of their expression and secondary metabolite accumulation.

ent-Copalyl diphosphate synthase (12 unigenes) and *ent*-kaurene synthase (8 unigenes) were the most abundant genes in the *A. carmichaelii* transcriptome. These enzymes are key members of the diterpene synthase (diTPS) family. In *Salvia miltiorrhiza*, SmCPS and SmKSL catalyse the transformation of GGPP into miltiradiene in a stepwise fashion (Cheng *et al.*, 2013; Hao *et al.*, 2015). In *A. paniculata*, ApCPS2 can also catalyse the conversion of (E,E,E)-geranylgeranyl diphosphate (GGPP) (Garg *et al.*, 2015). Similar to ApCPSs, c70404.graph_c2 and c86542.graph_c0 were preferentially expressed in *A. carmichaelii* leaves. However, 7 of the 12 CPSs were not transcribed in the leaves, and c110247.graph_c0 and c35028.graph_c1 were only detected in the lateral roots and reproductive organs, respectively, implying that these genes might play diverse roles along with secondary metabolite accumulation in different *A. carmichaelii* organs. Distinct biological roles of CPS genes have been verified in some plants, such as *Oryza sativa*, in which OsCPS1 mainly localize to vascular bundle tissues, similar to *Arabidopsis* CPS, which is responsible for GA biosynthesis. In contrast, OsCPS2 transcripts mainly localize to epidermal cells involved in the response to environmental stressors, such as pathogen attack (Toyomasu *et al.*, 2015).

In flowering plants, the *ent*-kaurene synthases are bifunctional or monofunctional. As an example of bifunctionality, rice OsKSL2 catalyses the cyclization of *ent*-copalyl diphosphate into *ent*-beyerene as a major product and *ent*-kaurene as a minor product (Tezuka *et al.*, 2015). Regarding monofunctionality, the PtTPS19 enzyme of *Populus trichocarpa* exclusively produces *ent*-kaurene, while PtTPS20 mainly generates the diterpene alcohol 16 α -hydroxy-*ent*-kaurane (Irmisch *et al.*, 2015). In previous studies, the amino acid sequences of PtTPS19 and PtTPS20 have been shown to share high similarity (99.1%) and only one amino acid determines the product specificity of PtTPS19 and PtTPS20: a methionine (M) is present at position 607 in PtTPS19, whereas the smaller, more polar amino acid threonine (T) is located at this position in PtTPS20. Among the 8 KS (KSL) proteins in the *A. carmichaelii* transcriptome, c74022.graph_c0 and c85475.graph_c0 contain a class II TPS motif (DDXXD motif), and the FPKM analysis revealed the roots and leaves to be their predominant organs of distribution in this plant. In addition, their putative proteins displayed a methionine in the appropriate site, as observed in PtTPS19 of *P. trichocarpa*, indicating that *ent*-kaurene should be their catalysis product in *A. carmichaelii* plants.

In brief, the above unigenes comprise almost all known terpene biosynthesis pathway genes, and visibility play core roles to regulate the DDAs biosynthesis. They initiate the pathway network research for the terpenoid-alkaloids metabolites of *A. carmichaelii* plants. In addition, these candidate genes provide a better understanding of the molecular mechanisms responsible for the quality of this medicinal material.

Conclusion

This study produced the first transcriptomic dataset and provided a comprehensive pathway network for the terpenoid-alkaloids metabolites of *A. carmichaelii* plants, allowing us to efficiently identify candidate genes involved in the biosynthetic pathways of phenylpropanoids, alkaloids, and especially AC, HA and MA. Based on the results, we obtained a better understanding of the molecular mechanisms responsible for the quality of this medicinal material.

Acknowledgements

This work was supported by Science and Technology Support Program of Sichuan Province (No 2016JY0089 and 2017TD0001), Scientific Research Project of Sichuan Provincial Department of Education (No 16ZB0112), Key Research Project of National Natural Science Foundation of China (No 81630101), National Development and Reform Commission standardization project (No ZYBZH-C-SC-51), Scientific Research Funds of Chengdu University of Traditional Chinese Medicine (No 030029050 and ZRY1612) and the other foundations (No 2016ZY008 and 2015FY111500-140).

References

- Adiwilaga, K. and A. Kush, 1996. Cloning and characterization of cDNA encoding farnesyl diphosphate synthase from rubber tree (*Hevea brasiliensis*). *Plant Mol. Biol.*, 30: 935–946
- Beck, G., D. Coman, E. Herren, M.A. Ruiz-Sola, M. Rodriguez-Concepcion, W. Gruissem and E. Vranova, 2013. Characterization of the GGPP synthase gene family in *Arabidopsis thaliana*. *Plant Mol. Biol.*, 82: 393–416
- Chen, W., S. He, D. Liu, G.B. Patil, H. Zhai, F. Wang, T.J. Stephenson, Y. Wang, B. Wang, B. Valliyodan, H.T. Nguyen and Q. Liu, 2015. A sweetpotato geranylgeranyl pyrophosphate synthase gene, *IbGGPS*, increases carotenoid content and enhances osmotic stress tolerance in *Arabidopsis thaliana*. *PLoS One*, 10: e0137623
- Cheng, Q., Y. He, G. Li, Y. Liu, W. Gao and L. Huang, 2013. Effects of combined elicitors on tanshinone metabolic profiling and *SmCPS* expression in *Salvia miltiorrhiza* hairy root cultures. *Molecules*, 18: 7473–7485
- Ding, J.Y., X.X. Liu, D.M. Xiong, L.M. Ye and R.B. Chao, 2014. Simultaneous determination of thirteen aminoalcohol-diterpenoid alkaloids in the lateral roots of *Aconitum carmichaelii* by solid-phase extraction-liquid chromatography-tandem mass spectrometry. *Planta Med.*, 80: 723–731
- Ding, L.S., F.E. Wu and Y.Z. Chen, 1993. Diterpenoid alkaloids from *Aconitum gymnantrum* (In Chinese). *Yao xue xue bao = Acta Pharm. Sin.*, 28: 188–191
- Facchini, P.J., 2006. Regulation of alkaloid biosynthesis in plants. *Alkaloids Chem. Biol.*, 63: 1–44
- Gao, J.H., F.X. Hou, Y.T. Ma and C. Peng, 2018. Molecular phylogeny and population structure of *Aconitum carmichaelii* (Fuji) in Western China. *Intl. J. Agric. Biol.*, 20: 826–832
- Gao, J.P., D. Wang, L.Y. Cao and H.F. Sun, 2015. Transcriptome sequencing of *Codonopsis pilosula* and identification of candidate genes involved in polysaccharide biosynthesis. *PLoS One*, 10: e0117342
- Garg, A., L. Agrawal, R.C. Misra, S. Sharma and S. Ghosh, 2015. *Andrographis paniculata* transcriptome provides molecular insights into tissue-specific accumulation of medicinal diterpenes. *Bmc Genom.*, 16: 659
- Haas, B.J., A. Papanicolaou, M. Yassour, M. Grabherr, P.D. Blood, J. Bowden, M.B. Couger, D. Eccles, B. Li, M. Lieber, M.D. Macmanes, M. Ott, J. Orvis, N. Pochet, F. Strozzi, N. Weeks, R. Westerman, T. William, C. N. Dewey, R. Henschel, R.D. Leduc, N. Friedman and A. Regev, 2013. De novo transcript sequence reconstruction from RNA-seq using the Trinity platform for reference generation and analysis. *Nat. Protoc.*, 8: 1494–1512
- Hao, X., M. Shi, L. Cui, C. Xu, Y. Zhang and G. Kai, 2015. Effects of methyl jasmonate and salicylic acid on tanshinone production and biosynthetic gene expression in transgenic *Salvia miltiorrhiza* hairy roots. *Biotechnol. Appl. Biochem.*, 62: 24–31
- Irmisch, S., A.T. Muller, L. Schmidt, J. Gunther, J. Gershenzon and T.G. Kollner, 2015. One amino acid makes the difference: the formation of *ent*-kaurene and 16 α -hydroxy-*ent*-kaurene by diterpene synthases in poplar. *BMC Plant Biol.*, 15: 262
- Jaiswal, Y., Z. Liang, A. Ho, L. Wong, P. Yong, H. Chen and Z. Zhao, 2014. Distribution of toxic alkaloids in tissues from three herbal medicine *Aconitum* species using laser microdissection, UHPLC-QTOF MS and LC-MS/MS techniques. *Phytochemistry*, 107: 155–174
- Li, B. and C.N. Dewey, 2011. RSEM: accurate transcript quantification from RNA-Seq data with or without a reference genome. *BMC Bioinform.*, 12: 323
- Liu, X.X., X.X. Jian, X.F. Cai, R.B. Chao, Q.H. Chen, D.L. Chen, X.L. Wang and F.P. Wang, 2012. Cardioactive C(1)(9)-diterpenoid alkaloids from the lateral roots of *Aconitum carmichaelii* "Fu Zi". *Chem. Pharmac. Bull.*, 60: 144–149
- Manzano, D., P. Andrade, D. Caudepon, T. Altabella, M. Arro and A. Ferrer, 2016. Suppressing farnesyl diphosphate synthase alters chloroplast development and triggers sterol-dependent induction of jasmonate- and Fe-related responses. *Plant Physiol.*, 172: 93–117
- Mortazavi, A., B.A. Williams, K. McCue, L. Schaeffer and B. Wold, 2008. Mapping and quantifying mammalian transcriptomes by RNA-Seq. *Nat. Methods*, 5: 621–628
- Robinson, M.D., D.J. McCarthy and G.K. Smyth, 2010. edgeR: a Bioconductor package for differential expression analysis of digital gene expression data. *Bioinformatics*, 26: 139–140
- Ruiz-Sola, M.A., D. Coman, G. Beck, M.V. Barja, M. Colinas, A. Graf, R. Welsch, P. Rutimann, P. Buhmann, L. Bigler, W. Gruissem, M. Rodriguez-Concepcion and E. Vranova, 2016. *Arabidopsis* GERANYLGERANYL DIPHOSPHATE SYNTHASE 11 is a hub isozyme required for the production of most photosynthesis-related isoprenoids. *New Phytol.*, 209: 252–264
- Shim, S.H., S.Y. Lee, J.S. Kim, K.H. Son and S.S. Kang, 2005. Norditerpenoid alkaloids and other components from the processed tubers of *Aconitum carmichaelii*. *Arch. Pharm. Res.*, 28: 1239–1243
- Singhuber, J., M. Zhu, S. Prinz and B. Kopp, 2009. Aconitum in traditional Chinese medicine: a valuable drug or an unpredictable risk? *J. Ethnopharmacol.*, 126: 18–30
- Tai, C.J., M. El-Shazly, T.Y. Wu, K.T. Lee, D. Csupor, J. Hohmann, F.R. Chang and Y.C. Wu, 2015. Clinical aspects of aconitum preparations. *Planta Med.*, 81: 1017–1028
- Tang, X., Y. Xiao, T. Lv, F. Wang, Q. Zhu, T. Zheng and J. Yang, 2014. High-throughput sequencing and De Novo assembly of the *Isatis indigotica* transcriptome. *PLoS One*, 9: e102963

- Tezuka, D., A. Ito, W. Mitsuhashi, T. Toyomasu and R. Imai, 2015. The rice *ent-KAURENE SYNTHASE LIKE 2* encodes a functional ent-beyerene synthase. *Biochem. Biophys. Res. Commun.*, 460: 766–771
- Toyomasu, T., M. Usui, C. Sugawara, Y. Kanno, A. Sakai, H. Takahashi, M. Nakazono, M. Kuroda, K. Miyamoto, Y. Morimoto, W. Mitsuhashi, K. Okada, S. Yamaguchi and H. Yamane, 2015. Transcripts of two ent-copalyl diphosphate synthase genes differentially localize in rice plants according to their distinct biological roles. *J. Exp. Bot.*, 66: 369–376
- Wang, L., Z. Feng, X. Wang and X. Zhang, 2010. DEGseq: an R package for identifying differentially expressed genes from RNA-seq data. *Bioinformatics*, 26: 136–138
- Young, M.D., M.J. Wakefield, G.K. Smyth and A. Oshlack, 2010. Gene ontology analysis for RNA-seq: accounting for selection bias. *Genom. Biol.*, 11: R14
- Zhang, J., Y.L. Liu, X.M. Du, J.H. Zhao, J.H. Wang and Z.H. Li, 2018. Transcriptome and physiological analysis of germination in gibberellic acid-primed tobacco seeds. *Intl. J. Agric. Biol.*, 20: 1768–1778
- Zhang, J., Z.H. Huang, X.H. Qiu, Y.M. Yang, D.Y. Zhu and W. Xu, 2012. Neutral fragment filtering for rapid identification of new diester-diterpenoid alkaloids in roots of *Aconitum carmichaelii* by ultra-high-pressure liquid chromatography coupled with linear ion trap-orbitrap mass spectrometry. *PLoS One*, 7: e52352
- Zhang, M., P. Su, Y.J. Zhou, X.J. Wang, Y.J. Zhao, Y.J. Liu, Y.R. Tong, T.Y. Hu, L.Q. Huang and W. Gao, 2015. Identification of geranylgeranyl diphosphate synthase genes from *Tripterygium wilfordii*. *Plant Cell Rep.*, 34: 2179–2188
- Zhang, X., H. Guan, Z. Dai, J. Guo, Y. Shen, G. Cui, W. Gao and L. Huang, 2015a. Functional analysis of the isopentenyl diphosphate isomerase of *Salvia miltiorrhiza* via color complementation and RNA interference. *Molecules*, 20: 20206–20218
- Zhou, G., L. Tang, X. Zhou, T. Wang, Z. Kou and Z. Wang, 2015. A review on phytochemistry and pharmacological activities of the processed lateral root of *Aconitum carmichaelii* Debeaux. *J. Ethnopharmacol.*, 160: 173–193
- Zhu, X., X. Zeng, C. Sun and S. Chen, 2014. Biosynthetic pathway of terpenoid indole alkaloids in *Catharanthus roseus*. *Front. Med.*, 8: 285–293

[Received 24 Aug 2018; Accepted 06 Oct 2018; Published (online) 20 Aug 2019]